Journal of Alloys and Compounds 509 (2011) 10155–10160

Contents lists available at SciVerse ScienceDirect

Journal of Alloys and Compounds

journal homepage: www.elsevier.com/locate/jallcom

Sinterability and dielectric properties of $Ba_{0.55}Sr_{0.4}Ca_{0.05}TiO_3$–$CaTiSiO_5$–$Mg_2TiO_4$ composite ceramics

Qianqian Jia, Huiming Ji*, Xiaolei Li, Shan Liu, Zhengguo Jin

Key Laboratory for Advanced Ceramics and Machining Technology of Ministry of Education, School of Materials Science and Engineering, Tianjin University, No. 92 Weijin Road, Tianjin 300072, PR China

ARTICLE INFO

Article history:
Received 10 June 2011
Received in revised form 14 August 2011
Accepted 16 August 2011
Available online 22 August 2011

Keywords:
$Ba_{0.55}Sr_{0.4}Ca_{0.05}TiO_3$
$CaTiSiO_5$
Sintering temperature
Composite ceramics
Dielectric property

ABSTRACT

The composite ceramics of $Ba_{0.55}Sr_{0.4}Ca_{0.05}TiO_3$–$CaTiSiO_5$–$Mg_2TiO_4$ (BSCT–CTS–MT) were prepared by the conventional solid-state route. The sintering performance, phase structures, morphologies, and dielectric properties of the composite ceramics were investigated. The BSCT–CTS–MT ceramics were sintered at 1100 °C and possessed dense microstructure. The dielectric constant was tailored from 1196 to 141 as the amount of Mg_2TiO_4 increased from 0 to 50 wt%. The dielectric constant and dielectric loss of 40 wt% $Ba_{0.55}Sr_{0.4}Ca_{0.05}TiO_3$–10 wt% $CaTiSiO_5$–50 wt% Mg_2TiO_4 was 141 and 0.0020, respectively, and the tunability was 8.64% under a DC electric field of 8.0 kV/cm. The Curie peaks were broadened and depressed after the addition of $CaTiSiO_5$. The optimistic dielectric properties made it a promising candidate for the application of tunable capacitors and phase shifters.

1. Introduction

In recent years, (Ba, Sr)TiO_3 (BST) solid solutions have attracted great attention as tunable materials in microwave tunable filed [1]. The dielectric properties of BST ceramics are required to be relatively low dielectric constant (<600), low dielectric loss ($<6\times10^{-3}$), less temperature dependence and high electric field tunability [2]. The high sintering temperature (1350 °C) [3] limits the application of BST on multilayer devices. Lots of researchers have fabricated BST-oxide composite ceramics with low dielectric constant, low dielectric loss and flat Curie peaks by mixing BST with non-ferroelectric oxides [4–7]. Among the oxides, Mg_2TiO_4 ($\varepsilon_r = 14$, $Q\times f\approx 150{,}000$ GHz, $\tau_f\approx -50$ ppm/°C) is a popular dielectric material applied at microwave frequencies [8,9]. Many researchers have fabricated BST–Mg_2TiO_4 composite ceramics with good dielectric properties [10,11]. However, the high sintering temperature of approximately 1400 °C needs to be lowered for the application on the LTCC technology [11]. Although nanometer powders prepared by liquid-phase methods [12–15] and sintering agents such as B_2O_3 [3], Si_2O_3 [16], and Li_2CO_3 [17,18] have been used to fabricate low-temperature sintering BST ceramics, reports on the low sintering BST–Mg_2TiO_4 composite system are rare so far. As was reported [19], the dielectric constant and loss tangent of $CaTiSiO_5$ are 45 and 5×10^{-4} measured at room temperature and 1 MHz, respectively. Its low dielectric constant and loss tangent make it available in diluting the ferroelectric response and improving dielectric constant temperature stability of BST ceramics. Moreover, $CaTiSiO_5$ is proved to be effective in reducing the sintering temperature of $Sr(Ti_{0.95}Zr_{0.05})O_3$ ceramics [20], and doping of Ca^{2+} can suppress the dielectric loss and the temperature dependence of BST [21]. Therefore, we choose $CaSiTiO_5$ for preparing $Ba_{0.55}Sr_{0.4}Ca_{0.05}TiO_3$–$CaTiSiO_5$–$Mg_2TiO_4$ (BSCT–CTS–MT) composite ceramics in order to enhance the sintering performance and dielectric properties of BST–Mg_2TiO_4 ceramics.

In this paper, (90 wt%-*x*) $Ba_{0.55}Sr_{0.4}Ca_{0.05}TiO_3$–10 wt% $CaTiSiO_5$-*x* Mg_2TiO_4 (*x* = 0, 10, 20, 30, 40, 50 wt%) composite ceramics and 50 wt% $Ba_{0.55}Sr_{0.4}Ca_{0.05}TiO_3$–50 wt% Mg_2TiO_4 for comparison were prepared by solid-state method. B_2O_3 and Li_2CO_3 were added as sintering aids [18]. The ceramics were sintered densely and then the microstructure and dielectric properties were investigated. The purpose of this work is to enhance the sintering property and the dielectric constant temperature stability of BST materials system, which also expresses low dielectric constant and loss and optimistic dielectric tunability.

2. Experimental process

$Ba_{0.55}Sr_{0.4}Ca_{0.05}TiO_3$ powders were firstly fabricated by chemical co-precipitation method. Then the powders were calcined in alumina crucible at 750 °C for 4 h in air. Mg_2TiO_4 and $CaTiSiO_5$ powders were prepared from MgO, TiO_2 and $CaCO_3$, SiO_2, TiO_2 by solid-state method at 1290 °C and 1050 °C, respectively. The

* Corresponding author. Tel.: +86 022 27890485.
E-mail address: jihuiming@tju.edu.cn (H. Ji).

0925-8388/$ – see front matter.
doi:10.1016/j.jallcom.2011.08.066

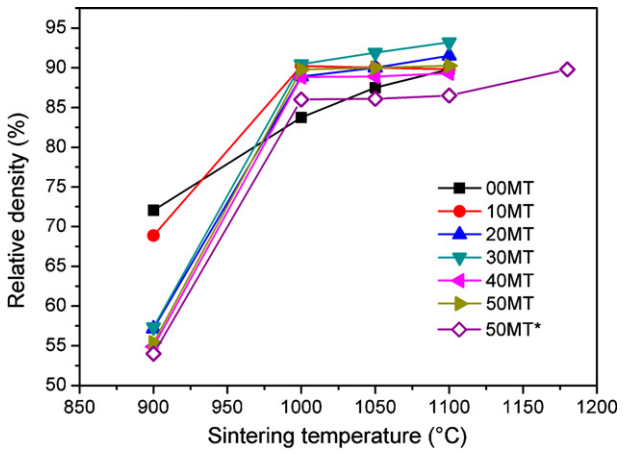

Fig. 1. The relative densities of BSCT–CTS–MT composite ceramics as a function of sintering temperatures.

composites of (90 wt%-x) $Ba_{0.55}Sr_{0.4}Ca_{0.05}TiO_3$–10 wt% $CaSiTiO_5$–xMg_2TiO_4 (x = 0, 10, 20, 30, 40, 50 wt%, signed as 00MT, 10MT, 20MT, 30MT, 40MT, and 50MT) and 50 wt% $Ba_{0.55}Sr_{0.4}Ca_{0.05}TiO_3$–50 wt% Mg_2TiO_4 (signed as 50MT*) with an addition of 0.75 wt% B_2O_3–3.75 wt% Li_2CO_3 were weighed and then ball-milled for 4 h and dried. The composite powders were added with 8 wt% methylcellulose binder and pressed into pellets. The composite samples were sintered at 900–1180 °C for 2 h.

The phases, morphologies, and elements were analyzed by Rigaku D/Max 2500V/PC X-ray diffractionmeter (XRD) with Cu Kα radiation, Hatchi S-4800 scanning electron microscope (SEM), and energy dispersive spectroscopy (EDS). The bulk densities of sintered samples were measured by Archimedes method. The relative densities are calculated by the formula $\rho_r = \rho_{bulk}/\rho_{theo} \times 100\%$, where ρ_r, ρ_{bulk}, and ρ_{theo} mean the relative density, bulk density, and X-ray theoretical density of the samples, respectively. The dielectric constant and dielectric loss of samples were measured using the Agilent E4980 LCR meter. The temperature dependences of dielectric constant were measured by high–low temperature incubator tank and YY2813 LCR meter at 1 MHz and a temperature range −55 to 125 °C. The tunabilities were tested by HM27004 C-T-V converter and YY2813 LCR meter at 1 MHz and room temperature.

3. Results and discussion

3.1. Sintering behaviors, phase structures and morphologies of BSCT–CTS–MT composite ceramics

The relative densities of BSCT–CTS–MT sintered at 900–1180 °C are shown in Fig. 1. It is clearly that the 00MT–50MT reach the relative density of 89.3–93.2% at 1100 °C, while 50MT* achieves its highest density at 1180 °C. The sintering temperatures are much lower than the pure BST ceramics (1350 °C) and BST–Mg_2TiO_4 composite ceramics (1400 °C). The nanometer $Ba_{0.55}Sr_{0.4}Ca_{0.05}TiO_3$ powders have high specific surface energy so that the ceramics could be sintered densely at a relatively lower temperature. With B_2O_3–Li_2CO_3 as sintering aids, the liquid-phase sintering mechanism takes effect during the sintering process. Moreover, the sintering temperature of 50MT is lower than 50MT*, which indicates the addition of $CaTiSiO_5$ promotes the sintering densification of BSCT–CTS–MT composite ceramics.

The XRD patterns of 00MT–50MT sintered at 1100 °C and 50MT* sintered at 1180 °C are shown in Fig. 2. A XRD pattern of pure $CaTiSiO_5$ is added in Fig. 2 (named Pure CTS). The $CaTiSiO_5$ phase is not detected in all of the patterns. For 00MT, a small amount of $Ba_2TiSi_2O_8$ is detected besides the perovskite structure $Ba_{0.6}Sr_{0.4}TiO_3$ phase. The absence of $CaTiSiO_5$ phase is possibly because $CaTiSiO_5$ reacts with $Ba_{0.55}Sr_{0.4}Ca_{0.05}TiO_3$ and generates the $Ba_2TiSi_2O_8$ phase. For 10MT, only the $Ba_{0.6}Sr_{0.4}TiO_3$ phase is detected, indicating that the $CaTiSiO_5$ and Mg_2TiO_4 react with $Ba_{0.55}Sr_{0.4}Ca_{0.05}TiO_3$ and the solid solution is formed, which has little impact on the perovskite structure of $Ba_{0.55}Sr_{0.4}Ca_{0.05}TiO_3$. The radius of Mg^{2+} (1.030 Å, CN = 12) is smaller than Ba^{2+} (1.610 Å, CN = 12) and Sr^{2+} (1.440 Å, CN = 12) [22], so it is easier for Mg^{2+} enters into the perovskite structure of $Ba_{0.55}Sr_{0.4}Ca_{0.05}TiO_3$. When the amount of Mg_2TiO_4 increases to 20 wt%, the new phase $BaMg_6Ti_6O_{19}$ appears. Mg_2TiO_4 may react with $Ba_{0.55}Sr_{0.4}Ca_{0.05}TiO_3$ and generate $BaMg_6Ti_6O_{19}$.

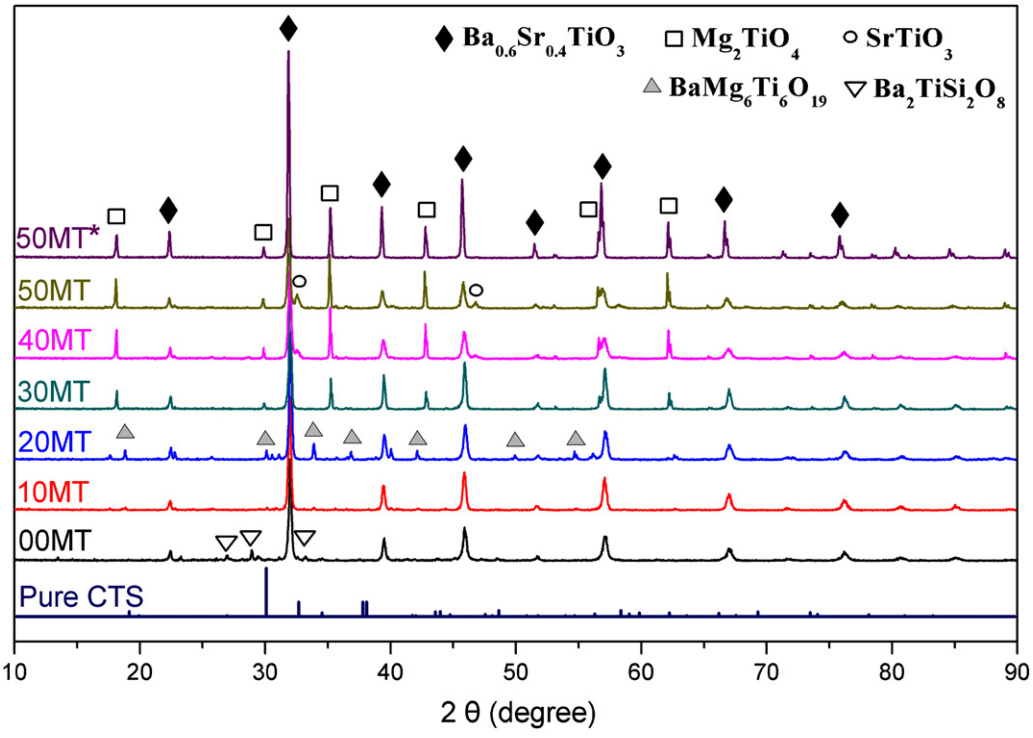

Fig. 2. XRD patterns of 00MT–50MT samples sintered at 1100 °C and 50MT* sintered at 1180 °C for 2 h.

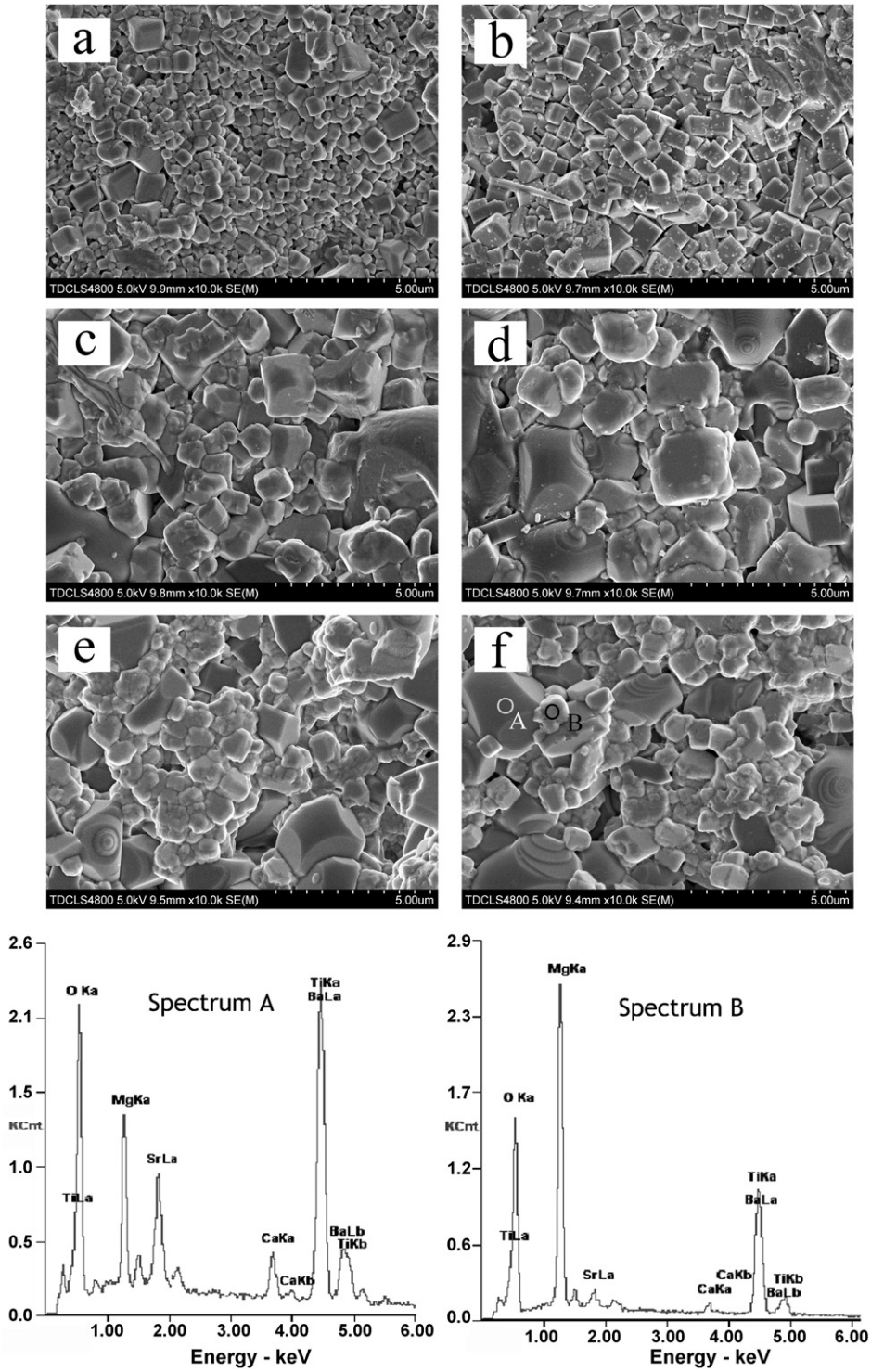

Fig. 3. SEM images of BSCT–CTS–MT composite ceramics and EDS spectra of 50MT ceramics sintered at 1100 °C for 2 h: (a) 00MT; (b) 10MT; (c) 20MT; (d) 30MT; (e) 40MT; (f) 50MT.

Furthermore, more than 30 wt% Mg_2TiO_4 is beyond the solution limit (~20 wt%), so there are $Ba_{0.6}Sr_{0.4}TiO_3$ and Mg_2TiO_4 phases and no other phases are observed. Since some Ba^{2+} ions remove from $Ba_{0.55}Sr_{0.4}Ca_{0.05}TiO_3$ lattice, small amount of $SrTiO_3$ is detected after 40 or 50 wt% Mg_2TiO_4 is added. The XRD pattern of 50MT* shows coexistence of $Ba_{0.6}Sr_{0.4}TiO_3$ and Mg_2TiO_4 without other phases, revealing that there is no obvious chemical reaction between $Ba_{0.55}Sr_{0.4}Ca_{0.05}TiO_3$ and Mg_2TiO_4.

The SEM images of BSCT–CTS–MT composite ceramics and EDS spectra of 50MT sintered at 1100 °C are displayed in Fig. 3. It is very clear that two component phases are co-existed and arrangement of grains is compact. EDS analysis in Fig. 3(f) shows that the dark grains with larger size marked as "A" are $Ba_{0.55}Sr_{0.4}Ca_{0.05}TiO_3$ and the light small grains marked as "B" are Mg_2TiO_4. Mg^{2+} is detected in the spectrum A, and Ba^{2+}, Sr^{2+}, and Ca^{2+} exist in the Mg_2TiO_4 grains, as shown in spectrum B. These ions may enter into the lattice

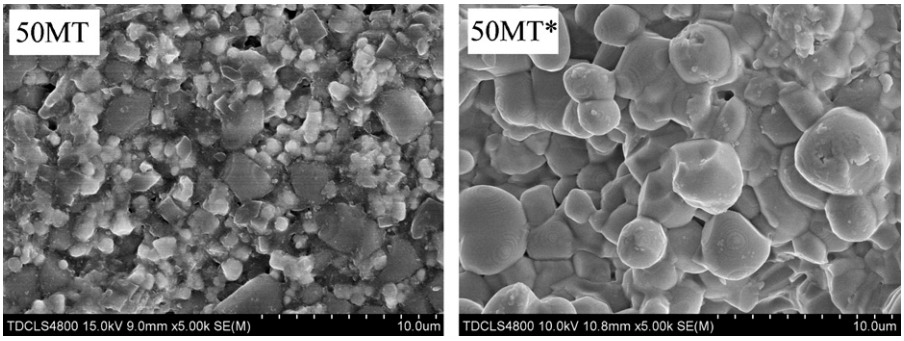

Fig. 4. SEM images of 50MT and 50MT* sintered at 1100 °C and 1180 °C for 2 h separately.

or exist on the surface of grains. As was reported, Mg^{2+} can easily substitute Ba^{2+} or Sr^{2+} of BST, and Mg^{2+} ions enter into *A* site of BST structure initially and then into the *B* site [9,10]. So it can be inferred that Mg^{2+} enters into the lattice of $Ba_{0.55}Sr_{0.4}Ca_{0.05}TiO_3$ grains. It can be proved in the XRD analysis in Fig. 2, in present study, the solubility limit of Mg_2TiO_4 is about 20 wt%. The $Ba_{0.55}Sr_{0.4}Ca_{0.05}TiO_3$ grain size increases from 0.5 to 2.5 μm with the increase of Mg_2TiO_4 content. The SEM images of 50MT and 50MT* sintered at 1100 °C and 1180 °C are shown in Fig. 4. The morphologies reveal that the Mg_2TiO_4 grains of 50MT grow larger after the addition of $CaTiSiO_5$ compared to 50MT*. We can conclude that the $CaTiSiO_5$ on the grain boundary prevents the growth of Mg_2TiO_4 grain and enhances the densification of BSCT–CTS–MT composite ceramics during the sintering process.

3.2. Dielectric properties of BSCT–CTS–MT composite ceramics

The dielectric properties of BSCT–CTS–MT composite ceramics measured at 20 °C and 2 MHz are summarized in Table 1. The dielectric constant is reduced from 1196 to 141 and the dielectric loss is reduced to the minimum value for 50MT. This reduction is attributed to the addition of dielectric materials Mg_2TiO_4 with low dielectric constant and loss tangent. Furthermore, the electrons are considered to be the cause of leakage loss, which plays an important role in the dielectric loss mechanism. Substitution of Ti^{4+} by Mg^{2+} would suppress formation of the Ti^{3+} so that fewer electrons are created during high temperature sintering, and the leakage loss is reduced as a result. The Curie temperature (T_c) which corresponds to the maximum value of dielectric constant shifts to higher temperature as Mg_2TiO_4 content increases. The shift of T_c results from three reasons. Firstly, below the solid solution limit of Mg^{2+} in BSCT, the substitutions of Mg^{2+} in the perovskite leads to change of *c*/*a* ratio and lattice constant of BST ceramics, which affects the T_c of composite ceramics. Secondly, the grain size of $Ba_{0.55}Sr_{0.4}Ca_{0.05}TiO_3$ increases from 0.5 to 3 μm with increase of Mg_2TiO_4 content. The increasing grain size results in decrease of internal stress [9], and T_c shifts to higher temperature. Thirdly, the BST ceramics are solid-state solution of barium titanate and strontium titanate, where a tetragonal ferroelectric phase and a cubic paraelectric phase exist at room temperature. There may be a compositional heterogeneity on microscopic scale in the specimens due to the co-existence of Ba^{2+} and Sr^{2+} at the *A*-site of perovskite structure [23]. The heterogeneity leads to a composition fluctuation in the phase transition temperature, which causes the slightly shift of T_c. The temperature dependences of dielectric constant for BSCT–CTS–MT composite ceramics measured at 1 MHz are given in Fig. 5. Samples exhibit the diffuse phase transition near Curie temperature and the Curie peaks are depressed and broadened with the containing of paraelectric Mg_2TiO_4 and $CaTiSiO_5$. According to the XRD results, the paraelectric phases such as $Ba_2TiSi_2O_8$, $BaMg_6Ti_6O_{19}$, Mg_2TiO_4, and $SrTiO_3$ dilute the ferroelectric response of BST ceramics, and more paraelectric phases lead to much flatter Curie peaks.

The tunability is determined by finding the change in dielectric constant at zero-field compared with those dielectric values when there is an applied electric field at room temperature using the formula:

$$\text{Tunability}\ (\%) = \frac{\varepsilon(E_0) - \varepsilon(E)}{\varepsilon(E_0)} \times 100\% \quad (1)$$

where $\varepsilon(E_0)$ is the zero-field dielectric constant and $\varepsilon(E)$ is the dielectric constant that results from an applied electric field of *E*. The tunabilities of BSCT–CTS–MT composite ceramics sintered at 1100 and 1180 °C at an applied field of 8.0 kV/cm are calculated according to formula (1) and presented in Table 1 and Fig. 6. The figure of merit (FOM) is defined as tunability/tan δ, which is

Table 1
The dielectric properties of BSCT–CTS–MT composite ceramics measured at room temperature (20 °C) and 2 MHz.

Samples	ε_r	tan δ	Tunability (8.0 kV/cm) (%)	Figure of merit (FOM)
	(at 2 MHz and room temperature)			
00MT	1196	0.0051	10.47	34.90
10MT	1106	0.0024	10.33	40.45
20MT	807	0.0031	8.58	34.32
30MT	1074	0.0027	9.67	35.81
40MT	368	0.0022	8.51	38.68
50MT	141	0.0020	8.64	43.20
50MT*	868	0.0031	19.24	62.06

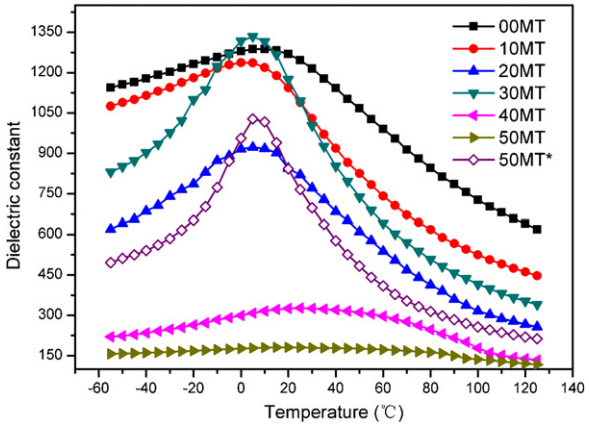

Fig. 5. The temperature dependence of dielectric constant of BSCT–CTS–MT composite ceramics measured at 1 MHz.

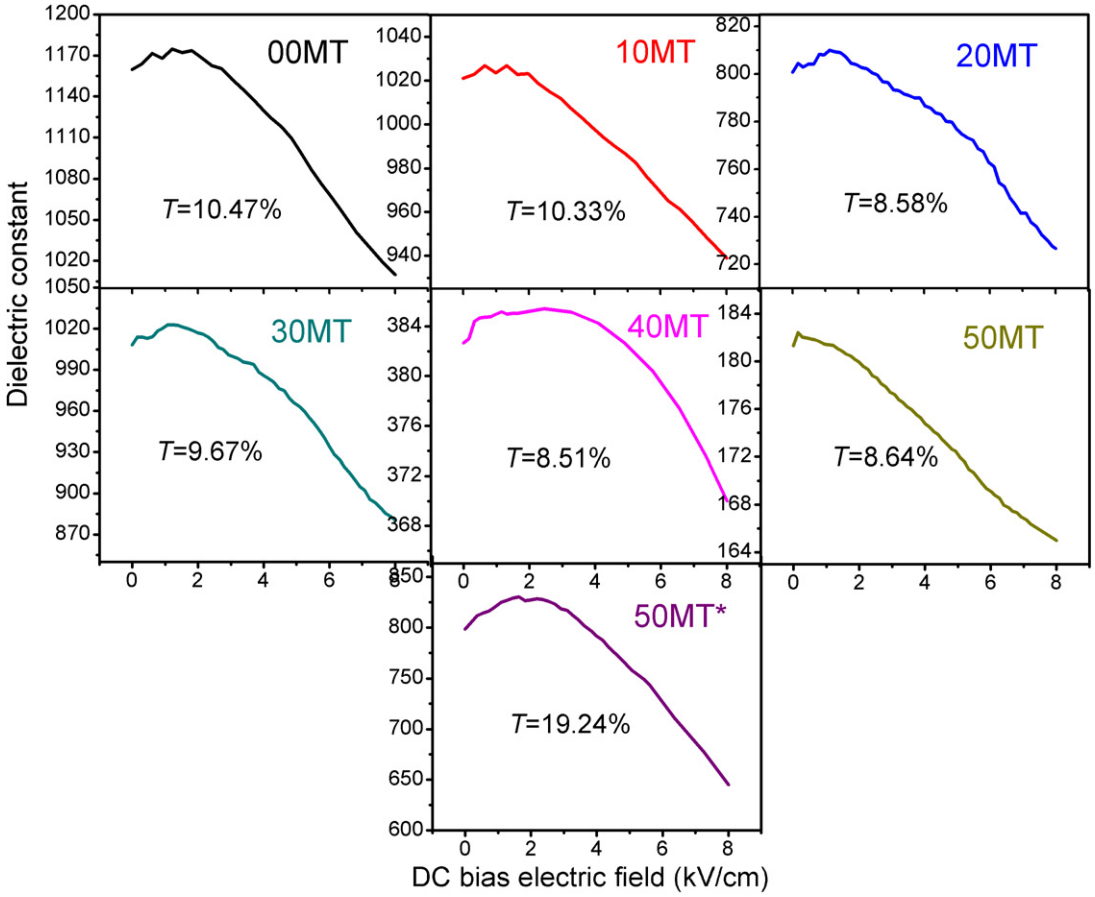

Fig. 6. The DC bias electric field dependence of dielectric constant of 00MT–50MT sintered at 1100 °C and 50MT* sintered at 1180 °C for 2 h.

usually used to characterize the overall dielectric performance of materials for tunable microwave devices [24]. The DC bias electric field dependence of dielectric constant of BSCT–CTS–MT composite ceramics is shown in Fig. 6. As we all know, the tunability of BST ceramics is associated with the anharmonic interactions of Ti^{4+} [25]. The addition of Mg_2TiO_4 does not break the connection of Ti–O–Ti bonds, which contributes to the high tunability of BSCT–CTS–MT composite ceramics. The tunability of 50MT* is much higher than the other samples, which indicates the addition of $CaTiSiO_5$ affects the anharmonic interactions of Ti^{4+}. The low loss and high tunability result in the high FOM value of 50MT and 50MT*. This kind of composite ceramics with low loss, high tunability, and excellent temperature stability has great potential for the application of tunable devices.

4. Conclusions

In this work, (90 wt%-x) $Ba_{0.55}Sr_{0.4}Ca_{0.05}TiO_3$–10 wt% $CaSiTiO_5$–xMg_2TiO_4 (x = 0, 10, 20, 30, 40, 50 wt%) composite ceramics were prepared by solid-state method. The BSCT–CTS–MT composite ceramics were sintered densely at 1100 °C, which was much lower than the sintering temperature of pure BST and BST–Mg_2TiO_4 composite ceramics. As the Mg_2TiO_4 content increased, the dielectric constant and dielectric loss decreased gradually. The Curie temperature shifted to higher temperature and the grain size increased dramatically. The addition of $CaTiSiO_5$ was proved to enhance the sintering property and lower the dielectric temperature dependence of composite ceramics. An optimum composite ceramic with dielectric constant 141, loss tangent 0.0020 at 2 MHz and 20 °C, tunability 8.64% under a DC electric field of 8.0 kV/cm and good temperature stability of dielectric constant was obtained. Both the low dielectric loss and enhanced tunable properties of BSCT–CTS–MT composite ceramics made them useful for microwave tunable applications.

References

[1] L.C. Sengupta, E. Ngo, J. Synowczynski, S. Sengupta, IEEE Trans. Microw. Theory 44 (1996) 845–849.
[2] L.C. Sengupta, S. Sengupta, IEEE Trans. Ultrason. Ferr. 44 (1997) 792–797.
[3] T. Hu, H. Jantunen, A. Unsimäki, S. Leppävuori, Mater. Sci. Semicond. Process. 5 (2003) 215–221.
[4] Y. Chen, X.-L. Dong, R.-H. Liang, J.-T. Li, Y.-L. Wang, J. Appl. Phys. 98 (2005) 064107.
[5] Y. Chen, Y.-Y. Zhang, X.-L. Dong, G.-S. Wang, F. Cao, J. Am. Ceram. Soc. 93 (2010) 161–166.
[6] K.B. Chong, L.B. Kong, L. Chen, L. Yan, C.Y. Tan, T. Yang, C.K. Ong, T. Osipowicz, J. Appl. Phys. 95 (2004) 1416–1419.
[7] M.W. Cole, E. Ngo, S. Hirsch, M.B. Okatan, S.P. Alpay, Appl. Phys. Lett. 92 (2008) 072906.
[8] H. Shin, H.-K. Shin, H.S. Jung, S.-Y. Cho, K.S. Hong, Mater. Res. Bull. 40 (2005) 2021–2028.
[9] X. Chou, J. Zhai, X. Yao, Appl. Phys. Lett. 91 (2007) 122908.
[10] P. Liu, J. Ma, L. Meng, J. Li, L. Ding, J. Wang, H.-W. Zhang, Mater. Chem. Phys. 114 (2009) 624–628.
[11] J.Y. Sun, X.J. Chou, J.W. Zhai, X. Yao, Ferroelectrics 356 (2007) 128–133.
[12] M.-L. Li, M.-X. Xu, J. Alloys Compd. 474 (2009) 311–315.
[13] Z. Wang, Y.-X. Li, Chin. Phys. Lett. 26 (2009) 117707.
[14] K.A. Razak, A. Asadov, J. Yoo, E. Haemmerle, W. Gao, J. Alloys Compd. 449 (2008) 19–23.
[15] V. Somani, S.J. Kalita, J. Electroceram. 18 (2007) 57–65.
[16] J.W. Zhai, X. Yao, X.G. Cheng, L.Y. Zhang, H. Chen, J. Mater. Sci. 37 (2002) 3739–3745.
[17] S.-H. Kim, J.-H. Koh, Microelectron. Eng. 87 (2010) 79–82.

[18] T. Hu, H. Jantunen, A. Deleniv, S. Leppävuori, S. Gevorgian, J. Am. Ceram. Soc. 87 (2004) 578–583.
[19] H. Taki, S. Hayakawa, US 3676351 1972-07-11.
[20] Z. Shen, H. Liu, Z. Wu, Z. Yao, M. Cao, D. Luo, Mater. Sci. Eng. B 136 (2007) 11–14.
[21] X.M. Chen, T. Wang, J. Li, Mater. Sci. Eng. B 113 (2004) 117–120.
[22] R.D. Shannon, Acta Crystallogr. A: Cryst. Phys. Diffr. Theor. Gen. Crystallogr. 32 (1976) 751–767.
[23] Q. Xu, X.-F. Zhang, Y.-H. Huang, W. Chen, H.-X. Liu, M. Chen, B.-H. Kim, J. Phys. Chem. Solids 71 (2010) 1550–1556.
[24] H.N. Al-Shareef, D. Dimos, M.V. Raymond, R.W. Schwartz, J. Electroceram. 1 (1997) 145–153.
[25] E.A. Nenasheva, N.F. Kartenko, I.M. Gaidamaka, O.N. Trubitsyna, S.S. Redozubov, A.I. Dedyk, A.D. Kanareykin, J. Eur. Ceram. Soc. 30 (2010) 395–400.